Structural Eng./Earthquake Eng., JSCE, Vol.17, No.1, 87s-103s, 2000 April

DAMPING PROPERTY OF PRESTRESSED CONCRETE CABLE-STAYED BRIDGES BASED ON MEASURED DATA

Tetsuo TAKEDA[1], Shin-ichi YAMANOBE[2] and Yuji NIIHARA[3]

[1]Member of JSCE, Senior Manager, Planning and Administration Office, Kajima Technical Research Institute (19-1, Tobitakyu 2-Chome, Chofu-shi, Tokyo 182-0036, Japan)
[2]Member of JSCE, M. Eng., Senior Research Engineer, Civil Eng. Dept., Kajima Technical Research Institute (19-1, Tobitakyu 2-Chome, Chofu-shi, Tokyo 182-0036, Japan)
[3]Member of JSCE, M. Eng., Research Engineer, Civil Eng. Dept., Kajima Technical Research Institute (19-1, Tobitakyu 2-Chome, Chofu-shi, Tokyo 182-0036, Japan)

In dynamic design of cable-stayed bridges, the evaluation of structural damping is important. As theoretical evaluation is difficult, however, it is usual to measure the damping ratio through vibration tests. The accumulated test data on PC cable-stayed bridges has been insufficient. In this study, the damping type, measurement method and evaluation method in seismic design are firstly reviewed, and the measured data from vibration tests are analyzed for recent PC cable-stayed bridges. The relation between damping ratio and natural frequency is studied, and the damping ratios of PC and steel cable-stayed bridges are compared. In addition, the damping characteristics during cantilever erection are investigated.

Key Words : *prestressed concrete cable-stayed bridge, damping ratio, seismic design, vibration test*

1. INTRODUCTION

Recently, the number of PC cable-stayed bridges has significantly increased. The bridge style is one of those oriented towards large bridges, and concrete is used as the main material. The Ikara bridge with a central span of 260m, which is the longest in Japan, and the 2-span Shin-inagawa bridge with a maximum span of 199m have been successively constructed, and the realizable span length has become close to that of steel cable-stayed bridges.

As PC cable-stayed bridges tend to be large, it has become more and more important to assure the safety of the bridge against earthquakes and wind loading. **Table 1** indicates examples of seismic design for large PC cable-stayed bridges in Japan. In the case of PC cable-stayed bridges, dynamic analysis has been applied to the design as it shows complicated behavior during earthquakes. Since the Hyogoken-Nanbu earthquake, "Specifications for Highway Bridges Part V: Seismic Design" has been revised, and the function of dynamic analysis in seismic design has been clearly indicated. Therefore, the dynamic analysis of PC cable-stayed bridges has become more and more important.

In designs based on dynamic analysis, the evaluation of structural damping is very important. Generally, structural damping is evaluated in the form of its modal damping ratio in dynamic design and field vibration tests, although damping characteristics depend on the structural members. Some theoretical studies have been challenged recently as observed in the study of Yamaguchi et al.[1]. Because theoretical evaluation of modal damping is difficult, however, the modal damping ratio is often measured through such field vibration tests at bridges in actual use. Up to now, many vibration tests have been performed and the measured data accumulated. However, many of them have not been performed systematically, and only the studies conducted by Kawashima et al.[2], Yamaguchi et al.[3] and Davenport et al.[4] have been statistically

This paper is translated into English from the Japanese paper, which originally appeared on J. Struct. Mech. Earthquake Eng., JSCE, No.626/I-48, pp.147-161, 1999.7.

Table 1 Seismic design examples of long-spanned PC cable-stayed bridges in Japan.

Bridge name (Year of completion)	Seismic design method
Ikara bridge (1996)	Seismic coefficient method Response spectrum method
Tokachi bridge (1995)	2-stage design. Material nonlinearity was considered in checking the ultimate horizontal strength during an earthquake
Shin-inagawa bridge (1998)	2-stage design. Nonlinear analysis considering variation of axial forces in the investigation using observed waves during Hyougoken-Nanbu earthquake.
Yobuko bridge (1989)	Seismic coefficient method Response spectrum method
Aomori Bay bridge (1992)	Seismic coefficient method Time-history response analysis and response spectrum method

Table 2 Type of vibration damping of structure.

Type of damping		Outline and features
Damping of material itself	Internal damping (Energy loss due to material itself)	This is energy loss due to nonlinearity, and is known as hysteresis damping when plasticity-induced damping is included. This kind of damping depends on vibration amplitude, but is almost independent of frequency.
Damping of structure system	Structural damping (Energy loss inside structure)	This is energy loss due to friction at bearings and joints, and depends on vibration amplitude. This kind of damping is almost independent of frequency.
	Dissipation damping (Dissipation of energy to outside of structure)	This is due to energy dissipation from the foundations to the surrounding subsoil and air resistance. This kind of damping depends on frequency, and is affected by the interaction between the foundations and soil.

summarized. In the above studies, data for steel cable-stayed bridges has been mainly used although those for PC ones has also been included. Since the previous studies, the measured damping data for PC cable-stayed bridges has increased, but the damping characteristics have not been fully clarified as PC cable-stayed bridges are relatively new. In Japan with its high seismic activity, seismic evaluations will be more and more important in order to construct larger PC cable-stayed bridges, and thus an understanding of their damping characteristics is absolutely indispensable.

In this study, the measurements from past vibration tests on damping characteristics of PC cable-stayed bridges are reviewed, and the damping behavior is studied in comparison with steel cable-stayed bridges. Firstly, kinds of damping, measuring methods and the evaluation in seismic design are briefly reviewed. Then the measured damping characteristics of the Ikara, Tokachi, Shin-inagawa, Yobuko and Aomori Bay bridges, which are all PC cable-stayed bridges that concerned the authors, are reported. Finally, the damping characteristics are statistically analyzed for the PC cable-stayed bridges for which vibration tests have been conducted, and the relationship with vibration mode and natural frequency is discussed. In this study, 16 PC cable-stayed bridges and 20 steel ones are investigated. Composite cable-stayed bridges were not considered although there is some measured data.

As for the parameters to indicate damping, the damping ratio h and logarithmic damping δ are often used. Generally, the damping ratio h is for seismic design and logarithmic damping δ for wind resistant design. The damping of bridges is very small, and the relation between the damping ratio h and logarithmic damping δ could be expressed by eq. (1).

$$\delta \approx 2\pi h \tag{1}$$

In this paper, the damping ratio h is adopted to evaluate damping characteristics.

2. DAMPING MEASURING METHODS

(1) Damping source and evaluation method in seismic design

As shown in **Table 2**, the damping of structures can be divided into the following three types according to their mechanism[5]: a) internal damping (or hysteresis damping), which is caused by the material itself; b) structural damping, which is by energy absorption inside the structure; and c) dissipation damping, which is from the dissipation of energy away from the structure. Internal damping consists of the following two parts: a) hysteresis damping caused by energy absorption due to a hysteresis loop of the stress-strain curve when plastic deformation occurs; and b) viscous damping of material, which exists even when behavior is linear. In the case of concrete, it is known that a hysteresis loop could be observed at extremely small levels of stress. Therefore it is generally accepted that hysteresis damping is the main component of internal damping, especially in the seismic design of concrete structures. Besides the above types of damping, there are also other types of damping, e.g., aerodynamic damping due to wind, system damping in cable-stayed bridges due to energy transferal between

Table 3 Reference value of damping ratio in "Specifications for Highway Bridges, Part V: Seismic Design".

Structural member	Linear case		Non-linear case	
	Steel structure	Concrete structure	Steel structure	Concrete structure
Superstructure	0.02～0.03	0.03～0.05	0.02～0.03	0.03～0.05
Rubber bearing	0.02		0.02	
Isolator	Equivalent damping ratio		Equivalent damping ratio	
Substructure	0.03～0.05	0.05～0.1	0.1～0.2	0.12～0.2
Foundation structure	0.1～0.3		0.2～0.4	

Table 4 Damping measuring method for bridge structure.

Vibrating the bridge artificially	Forced vibration method	Vibration is induced by exciter, and resonant curve is obtained. Damping ratio is computed using Half-Power method and modal circle curve fitting method.
	Free vibration method	Sudden stopping of exciter
		Manual vibrations
		Movement of vehicles
		Vertical motion of weight by crane
		Use of quick release jack
Naturally-induced Vibrations	Vibrations caused by Earthquakes and wind	System identification method, Random Decrement method
	Microtremor measuring method	Computed from Fourier spectra

cables and girders, and so on. The measured damping in vibration tests is a combination of the various aforementioned damping, and is often evaluated in the form of modal damping. It is very difficult to separate damping according to its mechanism. In seismic designs, damping is evaluated in the following way.

In the seismic design of highway bridges, the damping ratio is set for each member as indicated in **Table 3**, and then the modal damping is computed as strain energy proportional damping, according to the method shown in Specifications for Highway Bridges, Part V: Seismic Design[6]. For the superstructure of concrete bridges (main girders and main tower in PC cable-stayed bridges), the damping ratio is often set as h=0.03 in seismic designs, and therefore the computed damping ratio for the predominant vibration mode of superstructures using strain energy proportional damping is around 0.03 in most cases. The damping ratio of rubber bearings shown in **Table 3** is the equivalent damping ratio of linear rubber bearings, and any damping due to friction at moveable supports is not explicitly taken into account in the general design.

In the case of PC cable-stayed bridges, most measured damping ratios in field vibration tests for the predominant vibration mode of superstructures are smaller than those used in seismic design. However, as the vibration amplitude during earthquakes is large and internal damping and damping due to friction at the supports are added, the total damping is supposed to be around 0.03.

(2) Damping measurement methods

There are many kinds of methods to measure the damping of bridges. The methods used in the study are shown in **Table 4**, and can be divided into two categories, i.e., vibrating bridges using an exciter and observing damping during earthquakes or wind loading. In the latter case, the measured data are affected by the data processing method. When the microtremor measuring method is adopted, the measuring duration should be long and the measurements should be performed several times, and it is suggested that an averaging technique be used. The former type is more accurate, and can be divided into forced vibration tests and free vibration tests.

When the forced vibration test method is used, a vibration exciter is employed, and the exciting frequency is changed. The structure's response is observed, and the damping ratio is obtained from a resonant curve using the half-power method or modal circle curve fitting method. In the case of large PC cable-stayed bridges, a powerful exciter is required as the bridge is very heavy. In addition, a highly accurate vibration frequency setting is needed because the resonant curve is very sharp due to the small damping. However, the minimum frequency interval of exciters used for PC cable-stayed bridges is often around 0.01Hz, and it is difficult to assure sufficient measuring points around the peak when the half-power method is adopted.

On the other hand, in the case of free vibration tests, initial displacement is applied to the structure, and the damping ratio is computed from the observed waves of free vibration. In order to induce the initial displacement, the following ways are well adopted: a) sudden stopping of an exciter; b) movement of people or vehicles; c) vertical moving of a weight by crane; and d) quick releasing. The damping ratio could be directly observed and high accuracy could be achieved in this method, if it could result in a large initial displacement and a clear damping wave with

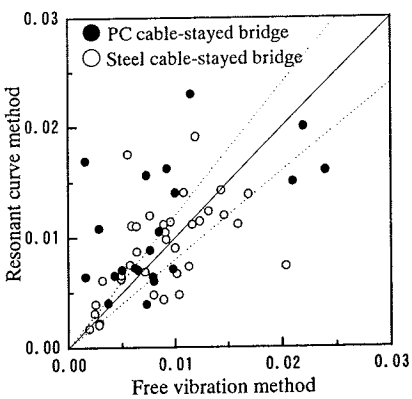

(a) Comparison of free vibration method and resonant curve method

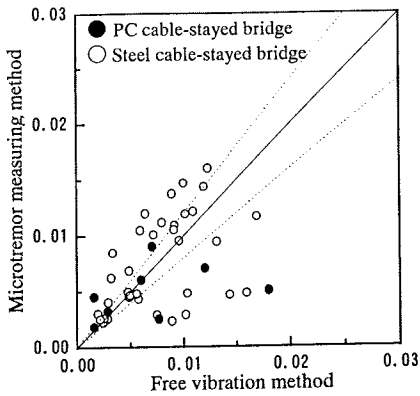

(b) Comparison of free vibration method and microtremor measuring method

Fig. 1 Dependence of damping ratio on test methods.

no oscillating disturbance could be obtained.

Among the bridges investigated in this study, there are some bridges where several types of measuring methods have been used to observe the damping ratio. **Fig.1** shows the comparison of observed results when different measuring methods were used. The horizontal axis indicates the damping ratio of free vibration tests, and the vertical axis the damping ratio of the resonant curve or that by microtremor measurement. The dotted lines show the range where the difference is within 20%. It can be seen that the damping ratio depends on the measuring method regardless of the type of bridge. In addition, it can not be confirmed from **Fig. 1**(b) that the damping ratio using the free vibration test is larger than that using the microtremor measurement, although the damping ratio is supposed to depend on the vibration amplitude. Therefore, in the evaluation of damping characteristics based on the measured data in many bridges, it is necessary to take care about the accuracy and equality of data.

3. DAMPING MEASUREMENT EXAMPLES OF LONG-SPANNED PC CABLE-STAYED BRIDGES

In this section, the measured damping characteristics of the Ikara, Tokachi, Shin-inagawa, Yobuko and Aomori Bay bridges are introduced.

(1) Ikara bridge

The Ikara bridge is a 5-span continuous PC cable-stayed bridge with a central span of 260m, which is shown in **Fig. 2**. In the bridge, forced vibration tests and microtremor measurements were conducted after the central span was closed[7]. The

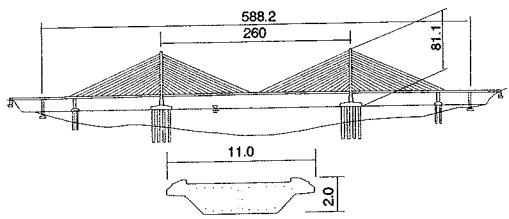

Fig. 2 Ikara bridge.

Table 5 Damping ratio of completed Ikara bridge through vibration test.

Vibration mode		Resonant curve	Micro-tremor
First out-of-plane symmetric	0.36Hz	0.0134	0.0094
First in-plane symmetric	0.37Hz	0.0119	0.0060
First in-plane asymmetric	0.48Hz	0.0067	-
Second in-plane symmetric	0.72Hz	0.0063	0069
Second in-plane asymmetric	0.89Hz	0.0050	0.0027

resonant curve obtained from forced vibration test and the transfer function computed using measurements of microtremors are shown in **Table 5**. For almost all modes, the damping ratio calculated from the resonant curve using the half-power method is larger than that obtained from measurements of microtremors.

As the bridge was constructed using the cantilever erection method, the gust response due to wind turbulence occurs easily during construction in the first mode, which is the mode in which displacement of the whole bridge is predominant. In order to mitigate the gust response of the main girder during cantilever erection, an active vibration control device using an active mass damper was developed and its effectiveness was verified[8]. The device was set on the end the main girder, and a vertical vibration was produced. The damping ratio was measured from free the vibration wave also. The vibration was generated by moving the weight vertically at the fundamental frequency of the bridge,

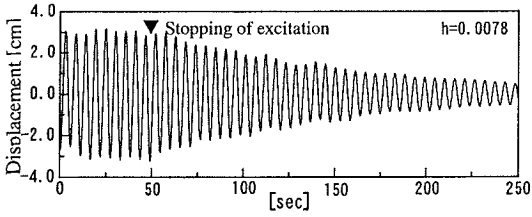

Fig. 3 Free vibration wave observed in vibration test at Ikara bridge during cantilever erection.

and a free vibration was produced by stopping the excitation once the vibration amplitude reached a certain level. **Fig. 3** shows the waveform of the free vibration. The damping ratio obtained was 0.0076～0.0078.

(2) Tokachi bridge

The Tokachi bridge is a 3-span continuous PC cable-stayed bridge with a central span of 251m, which is indicated in **Fig. 4**. The main girder is 32m wide, and the main tower is a single-column type. As it is constructed in the eastern region of Hokkaido, which is seismically active, and a single-column type main tower is adopted, the section force caused by seismic motion in the transverse direction could be significant. Therefore, a 2-stage seismic design was performed. At the bridge, forced vibration tests were conducted both during cantilever erection, and after the main girder was closed[9),10)]. Among the vibration tests conducted after the central closure of the main girder, the damping measuring test through impact excitation of vehicles and manually for an out-of-plane vibration of the single column tower are introduced in this subsection.

In the damping measuring test using impact excitation, an impact loading was applied by driving a truck over a difference in level on the deck, and then a free vibration wave induced by the impact was measured to obtain the damping ratio. When using this method, as several vibration modes were created, the measured waves were processed using a band-pass filter to distinguish waves for each mode. In the damping measuring test of the single column tower, the vibration was generated manually at the tower top. The measured damping ratios from the above tests are shown in **Table 6**. The damping ratios for the main girder were 0.0040～0.0050, and 0.0055～0.0059 for the main tower.

(3) Shin-inagawa bridge

The Shin-inagawa bridge is a 2-span continuous PC cable-stayed bridge with a maximum span of 198.7m as indicated in **Fig.5**. At the bridge, although vibration tests were not conducted after the closure

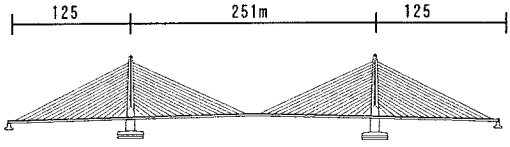

Fig. 4 Tokachi bridge.

Table 6 Damping ratio of Tokachi bridge.

Vibration mode		Damping ratio
First in-plane asymmetric	0.69Hz	0.0042～0.0048
Second in-plane symmetric	0.88Hz	0.0050
Second in-plane asymmetric	0.97Hz	0.0040
First out-of-plane mode of main tower	0.77Hz	0.0055～0.0059

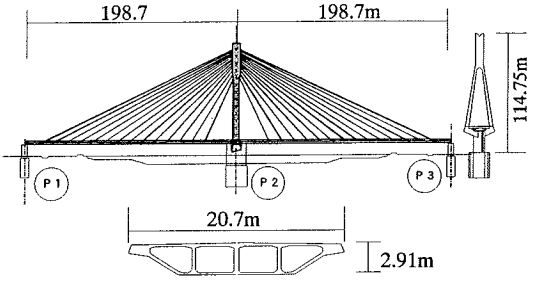

Fig. 5 Shin-inagawa bridge.

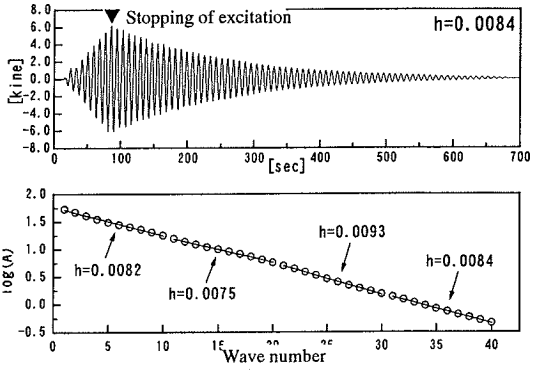

Fig. 6 Free vibration wave at Shin-inagawa bridge during cantilever erection.

of the main girder, they were performed by vertically moving a weight by crane once the cantilever length reached its maximum during cantilever erection[11)]. In the test, a weight of 4 tf (39 kN) was placed on the end of girder, and the vibration was created by lifting it up and lowering it at a fundamental frequency by a crane which was set on the girder at an approach part of bridge. The observed velocity wave of the main girder is shown in **Fig. 6**. Through the excitation, a vibration was generated with peak-to-peak amplitude of around 28cm at the end of the main girder. The damping ratio was 0.0084.

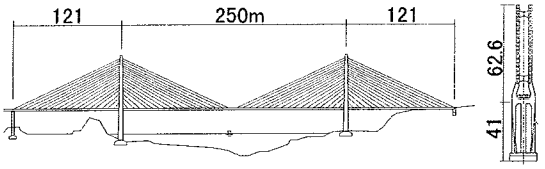

Fig. 7 Yobuko bridge.

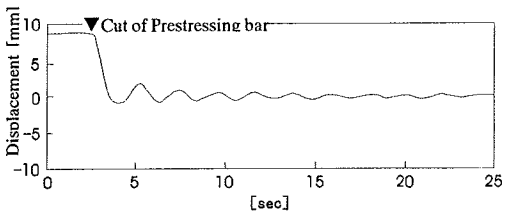

Fig. 8 Free vibration wave in longitudinal direction at main girder of Yobuko bridge.

It is generally known that the damping ratio depends on the vibration amplitude. At the bridge, as a clear waveform with a relatively large amplitude was obtained, the damping ratio was computed for 4 different time durations in order to observe the amplitude dependence of the damping ratio. However, no significant tendency was found because of the slight swell in the waveform. The damping ratio during cantilever erection does not include damping due to friction at the supports, and mainly consists of hysteresis damping of the concrete and dissipation damping from the foundations. At amplitudes of this order, the damping ratio does not depend on the vibration amplitude.

(4) Yobuko bridge

The Yobuko bridge is a 3-span continuous PC cable-stayed bridge with a central span of 250m, as shown in **Fig. 7**. At the bridge, forced vibration tests were performed after the closure of the main girder[12]. The damping ratios, which were computed from the resonant curve using the half-power method, were 0.008 for the first mode, and 0.0048～0.0064 for higher modes.

The Yobuko bridge is a floating type, where the main girder can move longitudinally. During earthquakes, the seismic force will exceed the friction at the supports on the end piers, and the main girder is supposed to vibrate as if on a swinging pole in the longitudinal direction. However, conventional exciters are not powerful enough at low frequency to cause a longitudinal vibration as above. At Yobuko bridge, a prestressing bar was temporarily fixed to one end part of the main girder, and pretension was applied from the abutment side. The free longitudinal vibration of the main girder like a swinging pole was generated by cutting the bar.

The free vibration wave is shown in **Fig. 8**. The frequency right after the release is close to the natural frequency of the model assuming movable supports, and that at a later stage is similar to the natural frequency of the model where complete adhesion is assumed at the supports. In seismic design, the damping due to friction at the supports is not considered. As shown by the measured waveform, however, the damping is significant, especially right after the release. In the test, although the damping ratio of the swinging-pole-mode was not computed, it was shown that damping due to friction at the supports was large, and that damping during earthquakes might be larger than that observed in vibration tests using an exciter.

(5) Aomori Bay bridge

The Aomori Bay bridge, as indicated in **Fig. 9**, is a 3-span continuous PC cable-stayed bridge with a central span of 240m. Vibration tests were not conducted at the bridge. However, earthquake observation has been performed after completion of the construction. The damping ratio has been computed from the observed earthquake responses during the Kushiro-Oki earthquake in 1993[13].

The simulation analysis of earthquake responses was conducted by applying earthquake motions observed at the bridge piers, and the responses at the superstructure were compared with observed ones. Rayleigh damping was assumed, and the damping ratio at the superstructures was determined so that the simulated and observed responses had the best agreement. **Fig. 10** indicates the comparison between the simulated and observed responses. A damping ratio of 0.02 leads to the best agreement between simulated and observed responses in the longitudinal direction for the first asymmetric mode (0.59Hz) and for the first symmetric mode (0.83Hz). This damping ratio is for the superstructure without taking into account the effects of cracks, and the dissipation damping to the subsoil is not included. The damping ratios of PC cable-stayed bridges measured through vibration tests are often small. However, it can be seen that the damping ratio during earthquakes is close to that used in seismic design when the response reaches a level of several tens–hundred gal.

As the capacity of the exciter is limited, it is almost impossible to cause sliding of the movable supports in vibration tests. At the Ikara and Yobuko bridges, the resonant frequency is close to the fundamental frequency of their models when complete adhesion is assumed at the supports. Therefore, it can be inferred that damping due to friction is not induced. As for the case when earthquakes of the level assumed in the design, sliding will occur at the supports, and damping due to

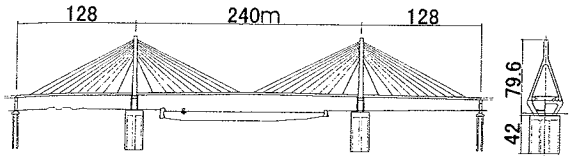

Fig. 9 Aomori Bay bridge.

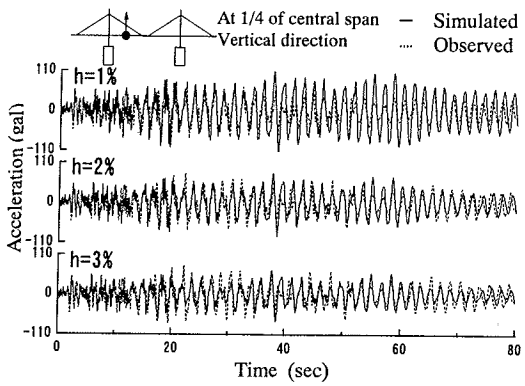

Fig. 10 Comparison between simulated and observed responses with focus on damping ratio. (Aomori Bay bridge)

friction will be induced. One of the reasons that the damping ratio during earthquakes at the level assumed in design is larger than that measured in vibration tests, is that damping due to friction at the supports is included.

4. DAMPING CHARACTERISTICS OF PC CABLE-STAYED BRIDGES

In this section, besides the above bridges, PC cable-stayed bridges where damping characteristics have been studied through vibration tests and other methods are also selected as investigation objectives, and the measurement obtained through a literature survey are statistically summarized. 16 bridges where damping characteristics were investigated are shown in **Table 7**. The measurement from 15 bridges were used for analysis, excluding the Aomori Bay bridge where damping was studied based on earthquake response observation.

There is both data computed using the half-power method from resonant curves and data obtained from free vibration waves. As was mentioned before, the latter data is more accurate, and therefore the damping ratios obtained from free vibration waves are given priority, and the observed data from resonant curve or microtremor measurements is only used when data from free vibration tests is not available. In addition, middle values are employed for some bridges when a range of damping ratios are indicated.

The damping characteristics of PC cable-stayed bridges are discussed in the following ways. Firstly, the maximum span length is used as a parameter and the overall tendency is studied in (1). Then, a detailed investigation concerning the vertical bending mode is performed in (2) and (3), as the corresponding data is relatively sufficient. In (4), a comparison between PC and steel cable-stayed bridges is performed. Finally, the damping characteristics during cantilever erection, which is a special structural type, are investigated in (5).

(1) Relation between the damping ratio and maximum span length

Among the PC cable-stayed bridges investigated in this study, most are 2 or 3-span ones although the number of spans varies from 1 to 5. **Fig. 11** shows the lower orders of vertical bending vibration modes for 2 and 3-span bridges. In the case of 3-span bridges where the main girder can move in the longitudinal direction, the lowest mode is a swinging pole vibration mode of the main girder in the longitudinal direction. However, this type of vibrations was not induced because the capacity of the exciter at low frequencies was insufficient. The damping ratio for the swinging pole mode was not observes in all bridges investigated in this study.

The relation between the damping ratio and the maximum span length of PC cable-stayed bridge is shown in **Fig. 12.** All the measured damping ratios after completion of construction are plotted, and averaging of data for each bridge is not conducted. From **Fig. 12**, the following approximate formula could be found representing the relation between the damping ratio h and maximum span length L.

$$h = 0.0757L^{-0.482}$$
(for all data) (2)

$$h = 0.0484L^{-0.388}$$
(for vertical bending vibrations) (3)

$$h = 1.248L^{-0.968}$$
(for vibrations in the transverse direction) (4)

$$h = 0.223L^{-0.824}$$
(for torsional vibrations) (5)

As the maximum span length increases, the damping ratio decreases for all vibration modes. It can also been seen that the damping ratio for the torsional mode is the smallest of the three types.

In addition, the damping ratios obtained by Kawashima et al. [2] from the data of 13 bridges (steel bridges: 10, PC bridges: [3] are also shown on the

Table 7 PC cable-stayed bridges where vibration tests have been performed.

Bridge name (Location)	Type	Span length / Width of girder (m)	Type of cable arrangement and number of stays / girder type	Vibration test method
Ikara bridge (Kagoshima Prefecture)	5-span continuous	44+120+260+120+ 44 / 11.0	Semi-harp type, double plane, 16 stays / Inversed-trapezoidal 2 boxes	Measurement of resonant curve using exciter, Microtremor measurement, Free vibration test during cantilever erection by AMD
Tokachi bridge (Hokkaido prefecture)	3-span continuous	125+251+125 32.8	Semi-harp type, double plane, 16 stays / Inversed-trapezoidal 4 boxes	Measurement of resonant curve through exciter, Microtremor measurement, Manual vibration, Free vibration test by movement of track
Yobuko bridge (Saga prefecture)		121+250+121 10.9	Semi-harp type, double plane, 17 stays / Inversed-trapezoidal 2 boxes	Measurement of resonant curve using exciter, Free vibration test in longitudinal direction by quick release of forced displacement
Aomori Bay bridge (Aomori prefecture)		128+240+128 25.0	Fan type, double plane, 10 stays / Inversed-trapezoidal 3 boxes	Identification of damping ratio using observed earthquake responses
Utagenka Bridge (Oita refecture)		61.05+170+61.05 14.9	Fan type, double plane, 12 stays / Separating 2 boxes	Measurement of resonant curve using exciter, Free vibration test by suddenly stopping exciter, Microtremor measurement during erection
Twinharp bridge (Hokkaido prefecture)		69.4+140+69.4 27.0	Harp type, single plane, 9 stays / 3 boxes	Measurement of resonant curve using exciter, Free vibration test by suddenly stopping exciter
Shin-ayabe bridge (Kyoto prefecture)		51.5+110+77.5 10.75	Fan type, double plane, 5 stays / Inversed-trapezoidal single box	Measurement of resonant curve using exciter, Free vibration test by suddenly stopping exciter, Microtremor measurement
Omotogawa bridge (Iwate prefecture)		46.65+85+46.65 7.0	Harp type, double plane, 5 stays / Single box	Measurement of resonant curve using exciter
Shin-inagawa bridge (Osaka prefecture)	2-span continuous	198.7+198.7 20.7	Fan type, double plane, 14 stays / Inversed-trapezoidal 3 boxes	Free vibration test during erection using weights
Shimamaruyama bridge (Mie prefecture)		113.4+113.4 11.5	Semi-harp type, double plane, 9 stays / Inversed-trapezoidal single box	Measurement of resonant curve using exciter, Free vibration test by suddenly stopping exciter
Fukiagehama-sunset bridge (Kagoshima prefecture)		94.3+94.3 6.8	Semi-fan type, double plane, 10 stays / Inversed-trapezoidal single box	Measurement of resonant curve using exciter, Free vibration test by suddenly stopping exciter
Koshiki-Daimyojin Bridge (Kagoshima Prefecture)		84.4+84.4	Semi-fan type, double plane, 7 stays	Free vibration test by movement of vehicles
Seiwun bridge (Hokkaido Prefecture)		53.5+53.5 5.4	Harp type, double plane, 4 stays / Edge girder	Measurement of resonant curve using exciter, Impact vibration test by dropping sand bags, Microtremor measurement, manual vibration test
Bungo bridge (Fukuoka prefecture)		37.45+37.45 16.8	Harp type, double plane, 3 stays / PC hollow slab	Measurement of resonant curve using exciter, Microtremor measurement
Matsugayama bridge (Kanagawa prefecture)	one-sided single span	96.6 4.2	Fan type, double plane, 4 stays / PC girder	Measurement of resonant curve using exciter
Yasuragi bridge (Toyama prefecture)		63.9 3.8	Fan type, double plane, 4 stays / PC girder	Free vibration test by movement of vehicles

same figure by dotted lines. The corresponding approximate formulas are as follows.

$$h = 0.649L^{-0.822} \quad \text{(for all data)} \tag{6}$$

$$h = 0.237L^{-0.645} \quad \text{(for vertical bending vibrations)} \tag{7}$$

$$h = 1.751L^{-0.990} \quad \text{(for vibrations in the transverse direction)} \tag{8}$$

$$h = 0.190L^{-0.638} \quad \text{(for torsional vibrations)} \tag{9}$$

The values from equations (2)-(5) are smaller than those from equations (6)-(9), which were obtained by Kawashima et al. In the formulas of Kawashima et al., the data used mainly consisted of the damping ratios for steel cable-stayed bridges. As described in (4), very large measured damping ratios of steel cable-stayed bridges with truss girder are also included.

(2) Damping characteristics of the vertical bending mode

As for the transverse mode and torsional mode, there are few measurement. In addition, such data is from bridges with different types of structures, and it is judged that an analysis of the two modes is difficult. On the other hand, more data was obtained for the vertical bending mode than those of the other two modes, and therefore further investigation is performed .

Except for single-span bridges, the 2 and 3-span

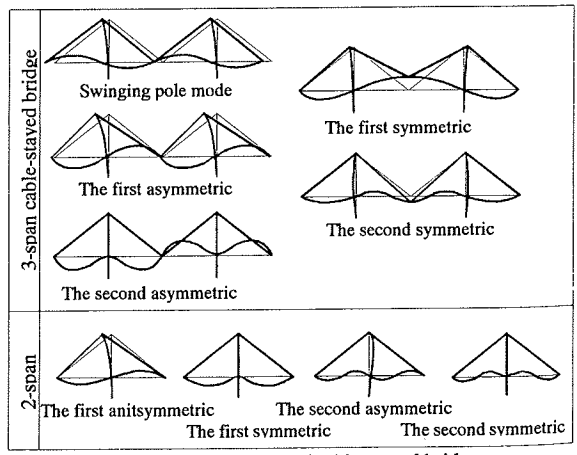

Fig. 11 Vibration modes of cable-stayed bridges.

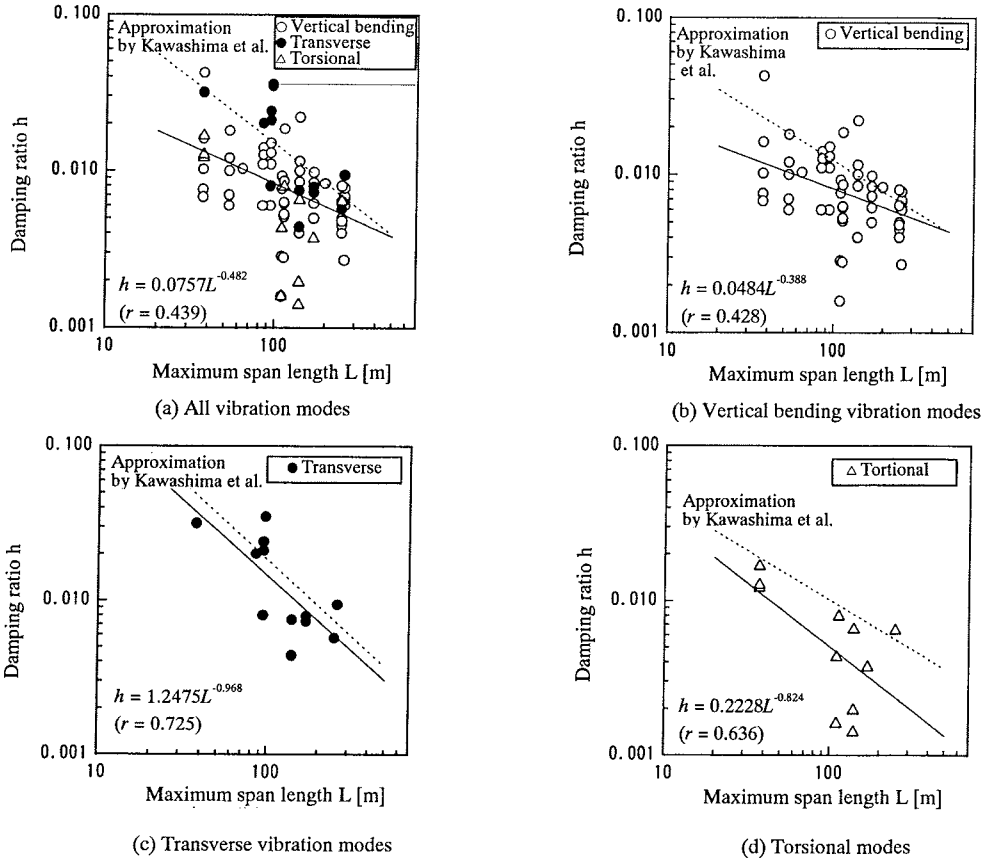

Fig. 12 Relation between damping ratio and maximum span length of PC cable-stayed bridges.

PC cable-stayed bridges are selected for the study of damping characteristics. Only the lower modes as shown in **Fig. 11**, which are important in the design, are studied.

The main factors affecting the damping ratio are as follows.

a) Structural type
Span arrangement (2-span, 3-span)
Cable layout
(single-plane cables, double-plane cables),
(fan type, harp type)
System for supporting the main girder
(floating, continuous girder, rigid connection)

b) Vibration mode and frequency
Vertical bending mode
(symmetric mode, asymmetric mode)
Transverse mode
(symmetric mode, asymmetric mode)
Torsional mode
(symmetric mode, asymmetric mode)
Frequency (order of mode)

c) Test and measuring methods
Resonant curve method
Free vibration method

d) Vibration amplitude
The amplitude difference caused by the capacity of exciters employed

e) Test conditions
With or without wind during test
Temperature during test (The change in tensile force of the cables affects the reaction force at the supports)

Among these factors, (c), (d) and (e) may cause large variations, and it is considered that an analysis on (a) and (b) could result in meaningful results for design.

It is considered that the cable layout has almost no effect on the damping of vertical bending mode, therefore this factor is not considered in the study. The data for single-plane types, of which there were few, are compared with those for double-plane types, and no notable differences are observed.

As for the supporting system for the main girder, bridges with rigid connections are all 2-span ones,

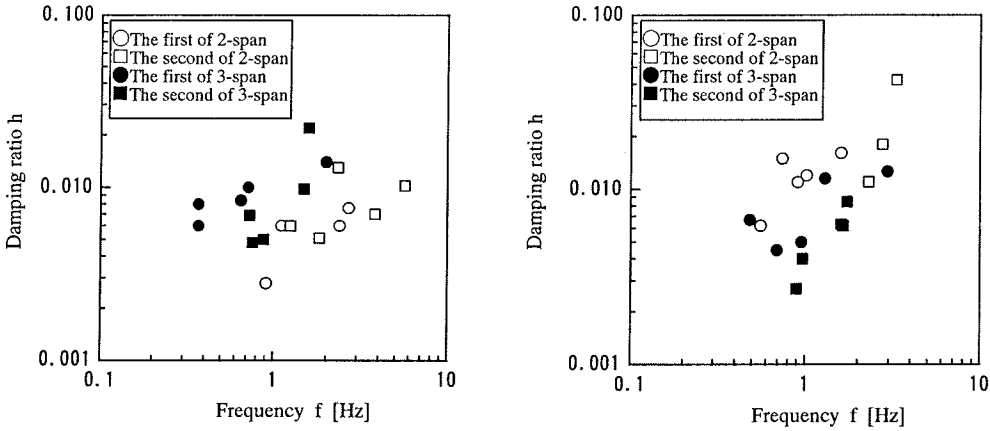

(a) Vertical bending symmetric modes (b) Vertical bending asymmetric modes

Fig. 13 Comparison of damping ratios of 2-span and 3-span bridges for vertical bending modes.

and therefore the data for 2-span bridges and that for 3-span bridges are separated from the start. In the case of the Ikara bridge which has 5 spans, its data are used in the analysis of 3-span bridges as it has two main towers. In the same way, data from the Shinayabe bridge which has 3 spans is adopted in the analysis of 2-span bridges because it has only one main tower. In addition, in the case where data for both 2 and 3-span bridges is analyzed, it is appropriate to use fundamental frequencies other than the maximum span length in order to evaluate the relation to the vibration mode. In the following discussion, the fundamental frequency is used as the parameter. The reasons are as follows. Dissipation damping from foundations to the subsoil depends on the frequency and tends to be larger as the frequency increases. The damping of cable-stayed bridges includes dissipation damping although its effect may not be very significant. In addition, the frequency dependence of damping is generally assumed in dynamic analysis using Rayleigh type or stiffness-proportional type damping. Therefore, the analyzed results using frequency as a parameter may easily be reflected in the dynamic analysis.

Fig. 13(a) and (b) indicate the analyzed results arranged for symmetric and asymmetric vertical bending modes, respectively. Data for cases where symmetric and asymmetric modes could not be separated are not included. In both modes, the damping ratio increases as the frequency increases. In the cases with symmetric modes, the damping ratios for 3-span bridges are larger than those for 2-span bridges. In the cases with asymmetric modes, the damping ratio for the second mode of the 3-span bridges is the smallest.

Considering the shape of the vibration modes, vertical bending modes could be divided into the

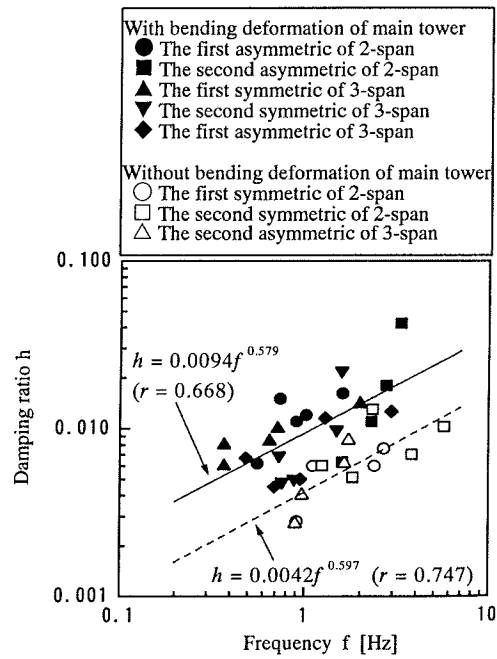

Fig. 14 Comparison of damping ratios for vertical bending modes with focus on bending deformation of the main tower.

following two types: a) vibration modes without bending deformation of the main tower (the first and second symmetric modes of 2-span bridges, and the second asymmetric mode of 3-span bridges); and b) vibration modes with bending deformation of the main tower (the first and second asymmetric modes of 2-span bridges, the first and second symmetric modes of 3-span bridges, and the first asymmetric mode of 3-span bridges). However, in the case of 3-span bridges, the ratio between the length of the side span and central span is not exactly 1:2 in most bridges, and the bending deformation of the main

tower did not vanish completely.

Fig. 14 shows the analyzed results arranged for the vibration modes with and without bending deformation of the main tower. The tendencies in both modes are quite similar, and the damping ratio for those modes with bending deformation of the main tower is larger than those without it. In the case without bending deformation of the main tower, the relation between damping ratio and frequency could be expressed using the following approximate formula.

$$h = 0.0042 f^{0.597} \tag{10}$$

In the same way, an approximate formula for the mode with bending deformation of the main tower could be found as follows. Compared with the above mode, the damping ratio for the mode with bending deformation of main tower is almost twice as large.

$$h = 0.0094 f^{0.579} \tag{11}$$

In the previous studies[3], the relation between the damping ratio and other factors for PC cable-stayed bridges has not been established. Through this study, it is confirmed that an incremental change in frequency leads to an incremental change in the damping ratio. The reasons could be considered as follows. In previous studies on PC cable-stayed bridges, 18 sets of data for vertical bending modes and 3 sets of data for torsional modes were available. In this study, 55 sets of data from 13 bridges for vertical bending modes, and 11 sets of data from 6 bridges for torsional modes are used. A clear relation could be observed because there is sufficient data.

The reasons why the damping ratio in the modes with bending deformation of the main tower is larger than those without it could be interpreted as follows.

In the PC cable-stayed bridges, the main tower is a RC structure, which is different from that of the main girder. Generally, the axial stress of the main tower is around several tens of kgf/cm^2 (several MPa) and vibration tests could be conducted right after completion of construction, when there should be no cracks in the main tower. Therefore, it is impossible for the damping ratio of the main tower to become larger than that of the PC main girder. In addition, as discussed in a later section, the tendency for the damping ratio of the mode with bending deformation of the main tower to be large could also be observed in cases of steel cable-stayed bridges. Therefore, large damping of the main tower cannot be considered as the reason for the large damping ratio in the mode with bending deformation of the main tower.

On the other hand, the mode with bending deformation of main tower is considered together with the rotational deformation (rocking) of the foundation. It has been demonstrated that the rotational deformation significantly affects the radiation damping from the foundation[14]. In the mode with bending deformation of the main tower, radiation damping due to rotation of the foundation is added to that caused by energy dissipation in the main girder, cables and main tower, which leads to a larger damping ratio.

Additionally, in the mode with bending deformation of the main tower, sliding occurs at all supports together with rotational deformation. It has been confirmed that the friction at the supports has a large effect on the damping ratio[15),16),17]. Among the data obtained from vibration tests of PC cable-stayed bridges in this study, the displacement of supports is unclear in almost all cases. However, it can be said that the friction at the supports affects the damping ratio obtained through vibration tests to a certain degree.

At this stage, it is difficult to identify which factor has the larger effect, out of radiation damping from the foundations and friction at the supports. However, it can be understood that both factors have a significant effect on the damping ratio, which leads to a larger damping ratio in the mode with bending deformation of the main tower. In addition, the reason for smaller damping in the torsional mode than those in other modes as shown in eq. (5) is interpreted as being because the torsional mode mainly consists of vibrations of the main girder and cable, and there is no bending deformation of the main tower.

(3) Damping ratio of the transverse vibration mode

Based on the above discussion results, the data for transverse vibrations is analyzed in this section.

Firstly, the measured damping ratios for transverse vibrations are compared with those from the approximate formulas for vertical bending modes with and without bending deformation of the main tower, as shown in **Fig. 15**. Although the data for transverse vibrations is significantly scattered, it can be observed that the damping ratio increases as the frequency increases, and is close to that of the approximate formula for the mode with bending deformation of the main tower. However, the damping ratio is relatively small for the first symmetric mode of the Twinharp bridge in the transverse direction. It has been reported that in the first symmetric mode of the Twinharp bridge in the

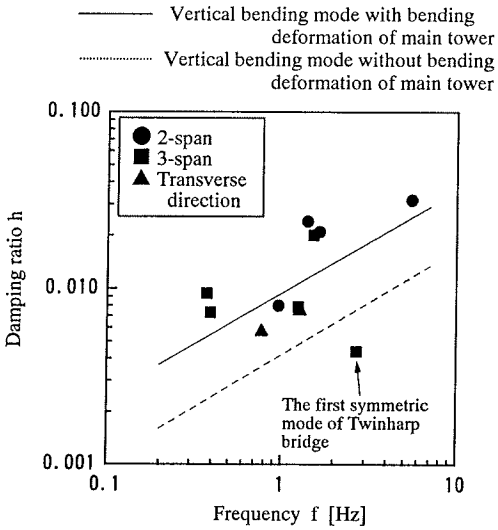

Fig. 15 Damping ratio for transverse modes.

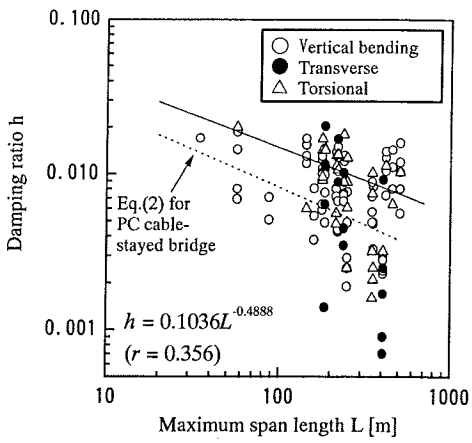

Fig. 16 Damping ratio and span length for steel cable-stayed Bridges.

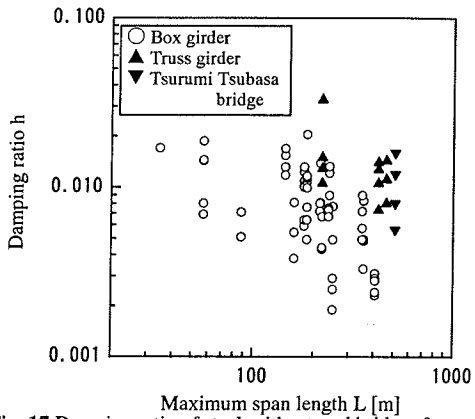

Fig. 17 Damping ratio of steel cable-stayed bridges for vertical bending vibration modes.

transverse direction, only the main girder of the central span showed significant deformation while the main tower showed almost no deformation[18]. As there is no rotational deformation of the foundations, it can be understood that the damping ratio is small compared with the others.

Next, the damping ratio for single-column towers in the transverse direction is discussed. As the damping that is added for transverse vibrations is small in the case of single-column towers, the earthquake resistance in the transverse direction is very important, and thus the evaluation of damping is an important key point. In this study, the PC cable-stayed bridges with single-column main towers are the Tokachi and Twinharp bridges.

In the Tokachi bridge, vibrations were induced manually, and the measured damping ratio is 0.0057. At the Twinharp bridge, the damping ratio is 0.0075, which is computed from the resonant curve. However, it has been suggested that the damping ratio obtained from the resonant curve might to be slightly exaggerated[18]. Taking the above into account, it can be said that the damping ratio for transverse vibrations of single-column towers is around 0.006～0.007.

This data is smaller than predicted using the approximate formula eq. (11) for the mode with bending deformation of the main tower. This is because the main girder has almost no deformation in the transverse vibration mode of the single-column main tower.

As described above, the tendency of the damping ratio in the transverse direction could be explained by considering the condition of bending deformation of the main tower in the vibration mode.

(4) Comparison of damping characteristics between PC and steel cable-stayed bridges

As for steel cable-stayed bridges, the data for 20 bridges obtained through a literature survey is used in this study.

Firstly, the general tendencies in PC and steel cable-stayed bridges are compared. The relations between damping ratio and maximum span length for vertical bending vibrations, transverse vibrations and torsional vibrations are shown in **Fig. 16**. As the scattering of data is significant, it is not easy to express it with an approximate formula. However, it can be seen that the damping ratio from the approximate formula in the figure is larger than that from eq. (2), which is for PC cable-stayed bridges. **Fig. 17** shows the damping ratios of vertical bending vibrations which are classified as steel box girders and steel truss girders, and those of the Tsurumi Tsubasa bridge. It can be observed that the damping

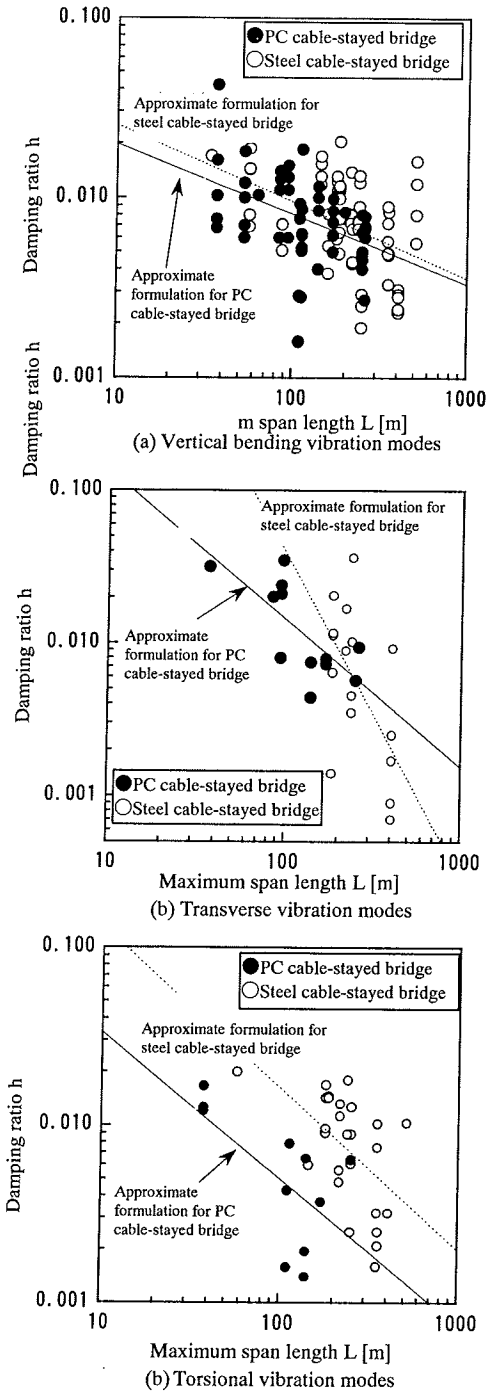

Fig. 18 Comparison of damping ratios of PC and Steel box girder cable-stayed bridges

ratios of bridges with steel truss girder are larger than those with steel box girder, which agrees to the results of Yamaguchi et al.[3]. As for the Tsurumi Tsubasa bridge, which has steel box girder, the damping ratios are larger than those of other bridges with steel box girder because of the frictional effects

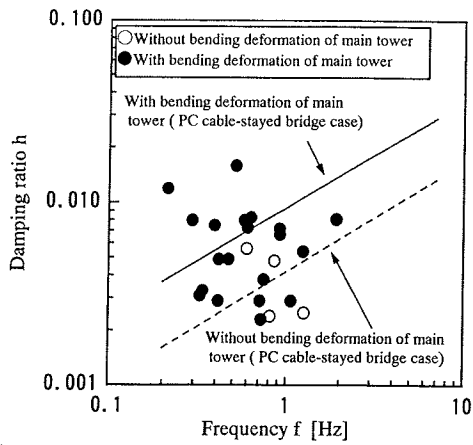

Fig. 19 Damping ratio of steel box girder cable-stayed bridges for vertical bending modes with and without bending deformation of main tower

Table 8 Frequency and damping ratio during cantilever erection

Bridge name	Frequency (Hz)	Damping ratio
Ikara bridge	0.130	0.0076～0.0078
Shin-inagawa bridge	0.116	0.0084

of the supports and cable dampers, as indicated by Yamaguchi et al.[19] As the maximum span length is long and the damping ratio is large in those bridges, this data has the effect that the approximate formula for steel cable-stayed bridges has a larger damping ratio. Therefore, in order to compare the damping of PC and steel cable-stayed bridges, only data for bridges with steel box girder is used next. However, the data for the Tsurumi Tsubasa bridge is also included.

Fig. 18 shows a comparison between the damping ratios of PC and steel cable-stayed bridges, using the above selected data. The maximum span length of PC cable-stayed bridges is shorter than those of steel ones, and it may be difficult to make direct comparisons. However, it can be said that the damping of PC cable-stayed bridges, which mainly consist of concrete materials, is not always larger than that of steel ones with steel box girder. With vertical bending vibrations and transverse vibrations, the damping ratios for the two types of bridges are almost the same. In terms of torsional vibrations, the damping of PC cable-stayed bridges tends to be rather smaller.

Fig. 19 shows the results corresponding to the vibration modes with and without bending deformation of the main tower, as in the case of PC cable-stayed bridges. Among the steel cable-stayed bridges on which vibration tests were conducted, there is no bridge with a symmetric continuous 2-span, and the amount of data for the vibration modes without bending deformation of the main tower is

small. However, it can be observed from the figure that in the case of steel cable-stayed bridges, the damping ratio for the mode with bending deformation of the main tower is also larger than that without bending deformation of the main tower. The approximate formulas eq. (10) and (11) of the damping ratios for the modes with and without bending deformation of the main tower in the case of PC cable-stayed bridges are shown in the same figure. It can be seen that they agree well with to the data for steel cable-stayed bridges.

The damping of PC cable-stayed bridges which mainly consist of concrete materials is not larger than that of steel ones with box girder. The reasons can be considered as follows.

Firstly, as described before, the damping due to friction at the supports and energy radiation from the foundations dominates the damping ratio, and therefore the effect of hysteresis damping, which depends on the type of materials, is insignificant. Secondly, PC cable-stayed bridges are very heavy, and large amplitude vibration tests are difficult to conduct. In the case of steel cable-stayed bridges like the Tsurumi Tsubasa bridge, vibration tests were conducted with such large amplitude that frictional damping occurred at the supports. Therefore, vibration amplitude is different in the two types of bridges. Compared to PC cable-stayed bridges, the effects of damping due to friction at the supports might be larger in steel cable-stayed bridges.

At this stage, it can not be concluded from the available measurement of vibration tests that damping of PC cable-stayed bridges is larger than that of steel ones with box girder.

(5) Damping characteristics of PC cable-stayed bridges during cantilever erection

PC cable-stayed bridges are unstable during cantilever erection. The construction time is short compared to the service time after completion, and thus there have been few studies on seismic behavior during construction. In the case of PC cable-stayed bridges, however, a much larger bridge may be constructed which requires a longer construction time, and thus seismic investigations during construction may become very necessary. In addition, gust responses are induced by wind turbulence easily, and wind resistance should be assured.

As for the vertical bending vibration mode during cantilever erection, the damping ratio was observed at the Ikara and Shin-inagawa bridges. The vibration amplitudes in both cases reached a certain level, and thus the data is very reliable. **Table 8** shows the measured results. Although the amount of data is insufficient and further accumulation of data is necessary, the following can be confirmed from the data.

During cantilever erection of PC cable-stayed bridges, there is no damping due to friction at the supports, and damping due to hysteresis damping of the concrete material and energy dissipation from the foundations dominates the damping behavior in the Ikara and Shin-inagawa bridges. From the measurements, it can be concluded that the damping ratio during cantilever erection is around 0.008, which is close to that of the bridge after completion of construction. When construction is complete, however, during earthquakes of the level assumed in the design, the vibration amplitude increases and damping due to friction at the supports may become large. Conversely, concerning the cantilever erection, even in cases with supports at the main tower, like 3-span bridges, the main girder is temporarily fixed to the top of the pier, and there is no frictional damping at the supports.

The measured damping ratio during cantilever erection is larger than that derived from approximate formula eq. (11) for the relation between the damping ratio and frequency for the mode with bending deformation of the main tower. This is because the rotational deformation during cantilever erection is larger than that of the completed bridge. In addition, the temporary member, especially for the main tower, is supposed to increase damping.

5. CONCLUSIONS

In order to clarify the damping characteristics of PC cable-stayed bridges, the measured damping data from vibration tests at 16 bridges are analyzed according to vibration mode and frequency, and damping characteristics are discussed. Concerning the damping characteristics of PC cable-stayed bridges, the following new findings are obtained.

(1) The damping ratio of PC cable-stayed bridges decreases as the maximum span length becomes larger. An approximate formula for each vibration mode has been established. The damping ratio of the torsional mode is smaller than those of the vertical bending and transverse modes.

(2) As for the vertical bending vibration mode, the measurements are analyzed according to whether the vibration mode is with or without bending deformation of the main tower, and an approximate formula between the damping ratio and frequency has been established. The tendencies of frequency dependence are similar in the two modes, and the damping ratio in the mode with bending deformation of the main tower is

Table 9 Steel cable-stayed bridges where vibration tests have been performed.

Bridge name (Location)	Type	Span length / Width of girder (m)	Type of cable arrangement and number of stays / girder type	Vibration test method
Onomichi bridge (Hiroshima prefecture)	3-span continuous	85+215+85 10.2	Radiation type, double plane, 2 stays / Two main girders of I shape	Measurement of resonant curve through exciter, Free vibration test by suddenly stopping exciter
Toyosato bridge (Osaka prefecture)		80.5+216+80.5	Fan type, single plane, 2 stays / Steel slab with box girder	Measurement of resonant curve using exciter, Free vibration test through movement of track
Arakawa bridge (Tokyo prefecture)		60.3+160+60.3 17.9	Harp type, single plane, 2 stays / Two girders of I shape and one box girder	Measurement of resonant curve using exciter, Free vibration test by suddenly stopping exciter
Kamome bridge (Osaka prefecture)		100+240+100 20.1	Multi-type, single plane, 10 stays / Steel slab with inversed-trapezoidal box	Free vibration test through movement of track, Shock vibration test using vehicles
Suehiro bridge (Tokushima prefecture)		110+250+110 18.5	Fan type, single plane, 2 stays / Inversed-trapezoid one box girder	Measurement of resonant curve using exciter, Free vibration test by suddenly stopping exciter
Tsurumi Tsubasa bridge (Kanagawa prefecture)		255+510+250 38.0	Multi-fan type, single plane, 17 stays / Flat box girder	Measurement of resonant curve using exciter, Free vibration test by suddenly stopping exciter
Sugawara Jhohoku Bridge (Osaka prefecture)		119+238+119 26.5	Fan type, single plane, 11 stays / Steel slab with inversed-trapezoidal box	Measurement of resonant curve using exciter, Free vibration test by suddenly stopping exciter
Yamatogawa bridge (Osaka prefecture)		149+355+149 30.0	Harp type, single plane, 4 stays / Box girder	Forced vibration by crane, Free vibration test through movement of track
Meiko-Nishi Bridge (Aichi prefecture)		175+405+175 16	Fan type, double plane, 12 stays / Flat hexagonal box	Measurement of resonant curve using exciter, Free vibration test by suddenly stopping exciter
Katsushika Harp bridge (Tokyo prefecture)		40.5+134+220 +60.5 / 25.7	Multi-fan type, single plane, 17+7 stays / Inversed-trapezoid 3 box	Measurement of resonant curve using exciter, Forced vibration by crane
Tenpozan bridge (Osaka prefecture)		170+350+120 39.25	Fan type, double plane, 9 stays / Flat hexagonal box	Measurement of resonant curve using exciter, Free vibration test through movement of track
Rokko bridge (Hyogo prefecture)		89.35+220+89.35 24.1	Fan type, double plane, 5 stays / Truss (composite steel slab with double decks)	Measurement of resonant curve using exciter, Free vibration test by suddenly stopping exciter, Shock vibration test using vehicles
Hitsuishi-Jima Bridge (Kagawa prefecture)		185+420+185 27.5	Multi-fan type, double plane, 11 stays / Truss (composite steel slab with double decks)	Measurement of resonant curve using exciter, Free vibration test by suddenly stopping exciter
Yokohama Bay bridge (Kanagawa prefecture)		200+460+200 40.2	Fan type, double plane, 11 stays / Truss (composite steel slab with double decks)	Measurement of resonant curve using exciter, Free vibration test by suddenly stopping exciter
Suigo bridge (Chiba prefecture)	2-span continuous	178.85+111.6 20.5	Harp type, single plane, 3 stays / Steel slab with inversed- trapezoidal box	Measurement of resonant curve using exciter, Free vibration test by suddenly stopping exciter
Aratsu bridge (Fukuoka prefecture)		185+115+45 21	Fan type, single plane, 13 stays / Steel slab with inversed-trapezoidal box	Measurement of resonant curve using exciter, Microtremor measurement
Yukitsuri bridge (Ishikawa prefecture)		44.4+57 3.5	Fan type, double plane, 5 stays / Flat hexagonal box	Shock vibration test by dropping weights, Manual vibration
Kawasaki bridge (Osaka prefecture)		87.5+40.65 3	Fan type, double plane, 6+4 stays / Flat hexagonal box	Manual vibration
Shinyo Country Club Sidewalk bridge (Gifu prefecture)		11+34.6 2.5	Radiation type, double plane, 1+2 stays / 3 boxes	Manual vibration
Gasyou bridge (Toyama prefecture)	2-span un-continuous	144+46+144 10.5	Fan type, double plane, 3 stays / Steel slab with 2 boxes	Measurement of resonant curve using exciter, Free vibration test through movement of track

Note: Although Katsushika bridge is a 4-span cable-stayed bridge, the data is classified into those of 3-span because it has two main towers. And although Aratsu cable-stayed bridge has 3 spans, its data are used for 2-span case as it has only one main tower.

about twice as large as that in the mode without bending deformation of the main tower. In the mode with bending deformation of the main tower, energy dissipation from the foundations is large, and damping due to friction at the supports caused by sliding deformation occurs. These are considered to lead to the large damping ratio in the mode.

(3) Concerning the damping ratio for transverse vibrations, as the amount of data is small and the scattering of data is significant, no clear tendency could be observed. However, it was confirmed that higher frequencies lead to larger damping ratios, which are close to those for the vertical bending vibration mode with bending deformation of the main tower.

(4) It can be confirmed that the damping ratio for the first transverse vibration mode of single column towers, which may undergo large seismic forces during earthquakes, is around $0.006 \sim 0.007$, although there is little data.

(5) Although PC cable-stayed bridges mainly consist of concrete materials, its damping ratio is not larger than that of steel cable-stayed bridges with box girder. The reasons can be considered as follows. Energy dissipation from the foundations and friction at the supports has a large effect on the damping ratio. In addition, PC bridges are very heavy, and the amplitude of vibration tests on PC bridges is small compared with that on steel bridges.

(6) As for cases of cantilever erection, there are only measurements from Ikara and Shin-inagawa bridges. However, the amplitudes of vibration tests at both bridges are sufficently large, and the data reliability is high. The damping ratio is

around 0.008, which is close to that of completed bridges. However, damping due to friction at the supports does not occur and thus the damping ratio will not increase as the amplitude increases. This tendency is different from that in completed bridges.

(7) The measured damping ratio through vibration tests is smaller than used in seismic design. However, as observed in earthquake records of Aomori Bay bridge, the damping ratio during earthquakes could reach 0.02. This is because damping due to friction at the supports during earthquakes is included, as observed in vibration tests at Yobuko bridge.

In this study, the damping characteristics of PC cable-stayed bridges are investigated based on the results of vibration tests. The measured damping ratios are significantly scattered, and are affected by the measuring method. It is necessary to accumulate further data through vibration tests with a high degree of accuracy.

In addition, as the effects of energy dissipation from the foundations and damping due to friction at the supports are significant in evaluating the damping ratio, it is necessary to conduct analysis to investigate these effects. The authors are continuing analytical investigation to evaluate the damping ratio.

ACKNOWLEDGMENTS: In this study, damping results from vibration tests attended by Kajima Technical Research Institute at Ikara bridge (Kagashima Prefecture), Tokachi bridge (Hokkaido Development Bureau), Shin-inagawa bridge (Hanshin Expressway Corporation), Yobuko bridge (Saga Prefecture) and Aomori Bay bridge (Aomori Prefecture), are reported. The authors would like to express their deep thanks to all participants. In addition, the authors would also like to thank Prof. Miki of Tokyo Institute of Technology for his precious advice.

APPENDIX A STEEL CABLE-STAYED BRIDGES WHERE VIBRATION TESTS HAVE BEEN PERFORMED

20 steel cable-stayed bridges where vibration tests have been performed are shown in **Table 9.**

REFERENCES

1) Yamaguchi, H., Takano, H., Ogasahara, M., Shimosato, T., Kato, M. and Kato, H.: Energy-based damping of cable-stayed bridges and its application to Tsurumi Tsubasa Bridge, *Proc. JSCE*, No. 543/I-36, pp.217-227, July, 1996.(in Japanese)

2) Kawashima, K., Unjoh, S. and Goda, Y.: A seismic design procedure of cable-stayed bridges, Part 1. Dynamic characteristics of cable-stayed bridges based on field vibration test results, *Report of Public Works Research Institute*, No.2388, June, 1986. (in Japanese)

3) Yamaguchi, H., Ito, M., Sakamoto, K. and Adikari, R.: Damping database of cable-stayed bridges and its analysis, *Journal of Constructional Steel*, Vol.1, July, 1993. (in Japanese)

4) Davenport, A. and Larose, G.: The structural damping of long-span bridges. An interpretation of observations, *Canada-Japan Workshop on Bridge Aerodynamics*, Ottawa, pp.111-118, September, 1989.

5) JSCE: Modification of "Standard specifications for design and construction of concrete structures", *Concrete Library 70*, pp.157-159, 1991. (in Japanese)

6) Japan Road Association: *Specifications for Highway Bridges, Part V: Seismic design*, December, 1996. (in Japanese)

7) Orita, H., Fukuda, H., Maeda, T. and Takeda, T.: Observation of wind response during construction and compulsory vibration tests after completion for Ikara Ohashi bridge, *Journal of the Japanese Society of Irrigation, Drainage and Reclamation Engineering*, Vol. 64, No.9, pp.921-926, September, 1996. (in Japanese)

8) Niihara, Y., Takeda, T., Oshio, M. and Nakano, R.: Vibration control of PC cable-stayed bridge during cantilever erection by AMD, *Proc. of the 5th Symposium on Developments in Prestressed Concrete*, pp.75-78, October,1995. (in Japanese)

9) Sato, M., Nagumo, H., Ohbo, N. and Inoue, M.: Vibration test of Tokachi bridge (PC cable-stayed bridge), *Proc. of the 5th Symposium on Developments in Prestressed Concrete*, pp.53-58, October,1995. (in Japanese)

10) Sato, M., Kamiyama, S., Takeda, T. and Yamamura, M.: Seismic behavior of Tokachi bridge under construction and its earthquake observation system, *Proc. of the 4th Symposium on Developments in Prestressed Concrete*, pp.57-62, October,1994. (in Japanese)

11) Enomoto, S., Okuda, H., Niihara, Y. and Yamauchi, T.: Vibration characteristics of Shin-inagawa bridge under cantilever construction obtained by wind observation, *Proc. of the 8th Symposium on Developments in Prestressed Concrete*, October, pp.721-726, 1998. (in Japanese)

12) Kuga, N., Tokuyama, S., Takeda, T. and Hishiki, Y.: Dynamic tests at Yobuko bridge, *Bridge and Foundation Engineering*, 89-9, pp.31-36, September, 1989. (in Japanese)

13) Inatomi, T., Takeda, T., Ohbo, N. and Yamanobe, S.: Analysis of seismic response characteristics of PC cable-stayed bridge (Aomori Bay Bridge) using strong motion observation data, *Journal of Structure Engineering*, Vol. 40A, pp.967-978, March, 1994. (in Japanese)

14) Kawashima, K., Unjoh, S. and Tsunomoto, M.: Damping characteristics of cable-stayed bridges associated with energy dissipation from foundation, *Civil Engineering Journal*, Vol.32, No.9, pp.33-39, 1990. (in Japanese)

15) Kawashima, K. and Unjoh, S.: Damping characteristics of cable-stayed bridges associated with energy dissipation at movable supports, *Proc. of JSCE*, No.404/I-11, pp.145-152, April, 1989.
16) Nagai, K., Egusa, T. and Sasaki, N.: Damping characteristics of long span box girder bridge, *Journal of Civil Engineering Structure and Material*, No.3, pp.79-87, January, 1988. (in Japanese)
17) Yoneda, M.: Some considerations on damping characteristics of bridge structures due to Coulomb friction force at movable supports, *Proc. of JSCE*, No.492/VI-23, pp.137-145, June, 1994. (in Japanese)
18) Mukae, K., Fujita, M., Honma, H. and Kondo, S.: Vibration test on PC cable-stayed bridge having the stays of single plane anchored at the single shaft pylons, *Technical Reports of Research Laboratory of Sumitomo Construction Co., Ltd.*, pp.71-79, 1992. (in Japanese)
19) Yamaguchi, H., Takano, H., Ogasawara, M. and Shimasato, T., Kato, M. and Okada, J.: Identification of dynamic characteristics by field vibration test in Tsurumi Tsubasa bridge, *Proc. of JSCE*, No.543/I-36, pp.247-248, July, 1996 (in Japanese)